Functionalization of hyaluronic acid hydrogels with ECM-derived peptides to control myoblast behavior

Juan Martin Silva Garcia[a], **Alyssa Panitch**[a,b], and **Prof. Sarah Calve**[a,*]

[a]Weldon School of Biomedical Engineering, Purdue University, 206 S. Martin Jischke Dr., West Lafayette, IN, 47907, U.S.A.

[b]Department of Biomedical Engineering, University of California – Davis, 451 E. Health Sciences Drive, Davis, CA, 95616, U.S.A.

Abstract

Volumetric muscle loss (VML) occurs when skeletal muscle injury is too large for the body to fully self-repair. Typically, fibrotic tissue fills the void, which reduces muscle functionality and limb movement. Although a wide variety of natural and synthetic scaffolds have been studied with the purpose of providing the appropriate structural support, to date no scaffold has significantly restored muscle functionality after VML. Satellite cells, adult stem cells within the muscle capable of restoring smaller injuries, are sensitive to the stiffness and composition of the surrounding environment. Scaffolds that only address structural support are not sufficient to restore functionality and instead need to be designed to both promote satellite cell activation and prevent excessive fibroblast recruitment. The objective of this study was to design a scaffold that mimicked the regenerative environment and determine how the biomechanical properties differentially influence myogenic precursor and connective tissue cells. One of the main extracellular matrix (ECM) molecules upregulated during regeneration is hyaluronic acid (HA). Therefore, thiol-modified HA and poly(ethylene glycol) diacrylate hydrogels were generated and functionalized with peptides based on ECM known to influence regeneration, including fibronectin, laminin and tenascin-C. Scaffolds with different stiffness were created by varying HA content. The influence of HA stiffness and peptide functionalization on myogenic precursor and connective tissue cell proliferation, migration and gene expression was quantified. Our results indicated that HA hydrogels functionalized with the laminin peptide, IKVAV, show potential due to the enhanced promotion of myogenic cell behaviors including migration, proliferation and an increase in relevant transcription factors.
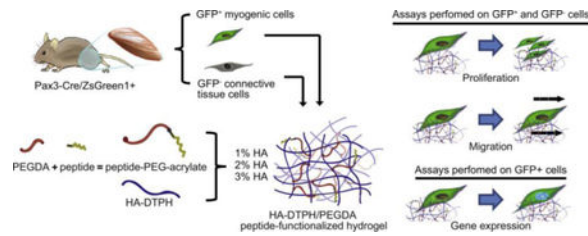
Graphical Abstract

*Corresponding Author: Prof. Sarah Calve, Tel: (765) 496-1768, Fax: (765) 494-0902, scalve@purdue.edu.

8.Conflicts of Interest

The authors declare no conflicts of interest.

1. Introduction

Mature myofibers and associated satellite cells are enclosed within a mesh-like basal lamina predominantly composed of type IV collagen and laminin [1]. Force generated by the myofibers is transmitted through the basal lamina to the surrounding connective tissues via type I and III collagen fibrils [2]. Capillaries, nerves, fibroblasts and other supporting cells reside between the myofibers within the interstitial space filled with hyaluronic acid (HA), fibronectin (FN) and assorted proteoglycans [3, 4].

The basal lamina regulates the spatiotemporal events during muscle regeneration. It facilitates regeneration by guiding activated satellite cells, or myogenic precursor cells (MPCs), to the site of injury, where laminin plays a significant role [1, 5, 6]. Additionally, it delimits connective tissue from the functional myofiber to reduce scar tissue formation [6]. HA, a large, linear glycosaminoglycan, is also significantly upregulated during muscle repair *in vivo* [7, 8] and *in vitro* studies demonstrated that HA upregulation promotes migration and reversibly suppresses differentiation [8–10]. Another potential key mediator of muscle formation is tenascin-C (TN-C). In homeostatic tissues, TN-C is restricted to areas of high loading, such as tendons and myotendinous junctions and is hypothesized to add mechanical stability [11]. Similar to HA, TN-C is upregulated in injured and regenerating skeletal muscle and thought to decrease cell adhesion, promote migration and inhibit premature fusion [7, 8, 12]. In addition, FN is upregulated and thought to act as a framework to enable MPCs, to migrate into and within the muscle injury [13]. During the later stages of myogenesis an intact basal lamina is reformed [14].

Although the skeletal muscle regenerative response is highly effective for minor injuries, this process is dramatically hindered for severe trauma [15]. Large volume injuries, known as volumetric muscle loss (VML), are characterized by the loss of basal lamina, and the inability to regenerate [16, 17]. Although fibroblasts also play a role in the initial regenerative response, over proliferation accompanied with pro-fibrotic cytokine expression causes the deposition of excessive collagen I and collagen III at the site of injury [18, 19]. The excessive fibroblast response, common in injuries where the basal lamina has been lost, disrupts the regenerative process and reduces muscle functionality and limb movement [20].

More than 70% of total war injuries result in VML [21]. For civilians, the most common causes are traumatic accidents, tumor ablation, and musculoskeletal diseases [17, 21].

Unfortunately for both populations, the current treatment consists of skeletal muscle transplantation, leading to harvest site morbidity [15, 22]. Although cell therapies have been investigated, the lack of ECM that supports a regenerative response at the site of injury results in poor cell integration [23]. To this end, a wide variety of synthetic materials and natural materials, including decellularized ECM-based scaffolds, have been tested with the purpose of providing the appropriate structural support that embedded myogenic cells need for muscle regeneration [24]. Although some promising results have been reported, to date there has been no complete restoration of VML [24]. Hence, it is clear that scaffolds need to be designed that better facilitate the recruitment of endogenous myogenic cells.

HA is a popular scaffold material for regeneration purposes among different tissues since it is biocompatible, facilitates diffusion of nutrients, and regulates tissue hydration [25]. Fabrication of HA-based scaffolds has been achieved through different chemical modifications usually targeting the carboxyl and hydroxyl groups of the disaccharide [25]. One modification method includes conjugation of dithiobis(propanoicdihydrazide) onto carboxylic acid moieties present in glucuronic acid of HA to produce thiolated HA [26]. After reducing disulfide bonds, free thiols enable crosslinking of HA chains using a linker such as poly(ethylene glycol diacrylate) (PEGDA). A Michael-type addition will rapidly occur at physiological pH and temperature between acrylates in PEGDA and free thiols [27]. PEGDA is hydrophilic, biocompatible and inert, making it a suitable cross-linker for engineered scaffolds [28]. Due to the inert nature of PEGDA, it does not degrade or promote protein adhesion [28]. In this system, HA can be degraded by hyaluronidases secreted by the embedded cells [26], which will allow for endogenous ECM to replace the temporary scaffold and promote muscle regeneration. While myogenic cells express the HA receptors CD44 and RHAMM [29], cell attachment is limited to cross-linked HA hydrogels due to the polyanionic nature of the surface [30].

To overcome the limited attachment of cells to PEGDA-HA-based scaffolds, peptides that support adhesion can be grafted into scaffolds. Although a fibronectin peptide, RGD, has been used in numerous biomaterial systems to promote cell adhesion [31], we wanted to investigate whether other ECM-derived peptides could better promote cell attachment of myogenic cells over connective tissue cells. The interaction of muscle-derived cells with HA-based scaffolds has been previously investigated in both 2D and 3D [32–37]. These scaffolds were either solely comprised of HA [32–34], or were combined with artificial polymers (poly(lactic) acid; [35]), gelatin [37] or the cell adhesion peptide RGD [36]. Two of these scaffolds, embedded with either adipose- or muscle-derived stem cells, were utilized to promote regeneration in mouse models, to limited success [32, 33]. Our approach to developing HA-based scaffolds is different in that we aim to identify the peptide sequence and hydrogel stiffness combinations that will enable us to direct muscle-derived cells towards cells with regenerating rather than homeostatic or fibrotic phenotypes. While the interaction of skeletal muscle with RGD-functionalized HA hydrogels has been investigated [36], none of the other peptides described in this study were studied in the context of both HA-based scaffolds and skeletal muscle-derived cells. Since the response of cells to variations in mechanics and ECM coating is dependent on lineage [38–40], it is necessary to investigate how both peptide functionalization and hydrogel stiffness combine to influence myogenesis.

With the long-term goal of engineering a scaffold that can preferentially recruit MPCs over connective tissue cells to promote VML repair, thiol-modified HA and PEGDA hydrogels were functionalized with ECM-derived peptides, including, RGD (found in FN and other ECM molecules), IKVAV (found in laminin) or VFDNFVLK (found in TN-C) [31, 41–43]. Scaffolds with storage moduli (G') ranging from to 400 Pa to 2 kPa were developed by increasing HA content of the hydrogel, and the *in vitro* effect of peptide type and hydrogel stiffness on satellite and connective tissue cells behavior was quantified.

2. Materials and methods

Unless otherwise specified, all reagents were of cell culture grade from ThermoFisher.

2.1 HA-DTPH synthesis

DTPH-modified HA was synthesized as described [44]. Briefly, 100 kDa sodium hyaluronate (Lifecore Biomedical) was dissolved at 10 mg/Ml in degassed Milli-Q water. Dithiobis(propanoicdihydrazide) (DTP; Frontier Scientific) was added at a molar ratio of 1 HA: 2 DTP while stirring. DTP was incorporated by activating the carboxyl group of β-D glucuronic acid of HA using (1-ethyl-3-(3-dimethylaminopropyl) carbodiimide (EDC) at a Ph of 4.75. The reaction was stopped after 1 h by increasing the Ph to 7 with the addition of 1 M sodium hydroxide (NaOH) so that 26% of the available glucoronate carboxyl groups were functionalized with a disulfide bond present in DTP.

The disulfide bond of DTP was reduced using dithiothreitol (DTT) at a molar ratio of 1 DTP: 5 DTT at a Ph of 8.5 for 24 h while stirring. The hyaluronic acid-dithiobis(propanoichydrazide) (HA-DTPH) solution was then transferred to a dialysis membrane (15 kDa cut-off) and dialyzed against a 0.3 Mm hydrogen chloride (HCl; Ph 3.5), with 100 Mm sodium chloride (NaCl), and the dialysis solution was replaced daily for 2 weeks. This was followed by dialysis against 0.3 Mm HCl (Ph 3.5) without NaCl, and the solution was replaced daily for 1 week. HA-DTPH solution was frozen at −80 °C, lyophilized and kept at −80°C for long-term storage and −20°C for a storage duration less than 2 weeks. The resulting free thiol content was measured using Ellman's method [45, 46]. The number of thiols per 100 disaccharide units of HA was calculated by dividing thiol molar concentration by non-thiolated HA molecular weight.

2.2 Hydrogel preparation

2.2.1 Peptide-PEGDA solutions—Stock solutions of peptide-free PEGDA at 1.78%, 3.56%, and 5.34% (w/v) were prepared in advanced DMEM (high glucose with sodium pyruvate, cat# 12491015). Except for IKVAV, 4 mM peptide stock solutions were made in Milli-Q water. 4 mM IKVAV stock solution was prepared in 20% acetic acid and adjusted to pH 8 by first dissolving IKVAV in 20% acetic acid (10% of final volume), then adding 10× PBS (10% of final volume). The pH was adjusted to 8 with 1 M NaOH and volume was adjusted with 1× PBS. Both PEGDA and peptide stock solutions were sterilized by filtration through a 0.22 μm syringe filter before use. Next, PEGDA was functionalized with one of the peptides listed in Table 1 to generate peptide-PEGDA. Peptide functionalization was performed via Michael-type addition between the terminal cysteine on the peptide (Table 1)

and one acrylate group on PEGDA at pH 7.4 for 40 min at 37 °C in a humidified 5% CO_2 incubator. Each stock solution was made at a working concentration of 294 μM, 558 μM, and 1,176 μM.

2.2.2. HA-DTPH solutions—HA-DTPH solutions were prepared by dissolving lyophilized HA-DTPH in advanced DMEM and the pH was adjusted to 7.4 by adding 1.0 M NaOH, yielding HA-DTPH working stock solutions of 2%, 4%, 6% (w/v). Each stock solution was sterilized by filtration through a 0.22 μm syringe filter.

2.2.3 Hydrogel preparation—Hydrogels were formed by crosslinking the electrophilic acrylate groups of PEGDA with the reduced thiols of the HA via Michael-type addition. Peptide-free PEGDA and peptide-PEGDA were added to HA-DTPH at a ratio of 1:1 and then mixed for 15 s to generate 1%, 2%, or 3% (w/v) HA hydrogels with a peptide end concentration of 0 μM, 147 μM, 294 μM or 588 μM. The final acrylates/thiols ratio (w/w) was 0.8. HA-DTPH/PEGDA solutions were quickly pipetted into a μ-slide angiogenesis slide (ibidi;10 μl per well for cell culture), 48 well plate (150 μl per well for gene expression analysis) or Teflon covered slide (200 μl for rheological testing) and incubated for 1 h (cell culture), or 5 h (gene expression and rheological testing) at 37°C in a humidified 5% CO_2 incubator. After gelation, HA hydrogels were swelled under the same incubation conditions for 15 h with the addition of advanced DMEM supplemented with 1% fetal bovine serum (FBS, Atlanta Biologicals), 1% L-Glutagro (Corning), and 1% Penicillin-Streptomycin before cell-based or rheology assays.

2.3 Rheological characterization

The viscoelastic mechanical properties of the hydrogels were measured with an AR2000 rheometer (TA Instruments) using a 20 mm diameter parallel plate geometry at a starting normal force of 1 N. The hydrogels were prepared, incubated and swelled as previously stated above. The linear range of the viscoelastic response was first measured with an angular frequency sweep ranging from 0.1 to 200 rad/s at 0.5% strain. The storage and loss moduli of the hydrogels were measured with an increasing oscillatory stress sweep from 0.1 Pa to 100 Pa at 1 rad/sec. Teflon slides were secured to the bottom plate with tape to prevent movement during the test.

2.4 Cryo-SEM

Differences in pore diameter between 1%, 2%, and 3% (w/v) HA hydrogels were visualized by cryo-scanning electron microscopy (cryo-SEM). Cryo-SEM was performed on a FEI NovaNanoSEM with a GATAN Alto 2500 cryo-system at the Purdue Life Science Microscopy Facility. HA-DTPH/PEGDA solutions were pipetted into a SEM stub adaptor and incubated for 1 h at 37 °C in a humidified 5% CO_2 incubator before swelling for 15 h. Individual samples were flash-frozen by immersion in liquid nitrogen and then fractured with a scalpel. Fractured samples were then lyophilized inside the cryo-system and sputtered with platinum. Images were taken at 5 kV with a spot size of 3 and 10,000× magnification. Pore diameter was calculated using FIJI (NIH).

2.5   In vitro cell expansion and cell culture

2.5.1   Primary isolation and cell culture—Murine experiments were approved by the Purdue Animal Care and Use Committee (PACUC; protocol #1209000723). PACUC ensures that all animal programs, procedures, and facilities at Purdue University adhere to the policies, recommendations, guidelines, and regulations of the USDA and the United States Public Health Service in accordance with the Animal Welfare Act and Purdue's Animal Welfare Assurance. Pax3-Cre [47] and ROSA-ZsGreen1 transgenic mice [48] were obtained from the Jackson Laboratory (Bar Harbor, ME, USA) and used to generate Pax3-Cre/ ZsGreen1[+] progeny in which the satellite cells are GFP[+].

Tibialis anterior (TA) muscles were harvested from 3–4 week old mice. Each pair of TA muscles were placed in a digestion solution consisting of advanced DMEM and 2 mg/ml collagenase type II (Worthington Biochemical). After incubation for 1–1.5 h in a shaking water bath at 37°C, the suspension was passed through a 70 μm strainer to remove debris and undigested tissue. To completely remove all collagenase type II, the cell suspension was centrifuged, supernatant aspirated and resuspended in growth medium [DMEM (high glucose with sodium pyruvate), supplemented with 10% FBS, 1% L-Glutagro, and 1% Penicillin-Streptomycin], two times. Cells were then plated in a 100 mm cell culture dish and expanded in growth medium at 37 °C in a humidified 5% CO_2 incubator.

The resulting cell population was composed of GFP[+] MPCs and GFP^{−} cells, the latter of which were predominantly fibroblasts. The heterogeneous population of cells was expanded until 80% confluent and then passaged by dissociating cell monolayers with 1.5 mL trypsin/ EDTA, centrifuged, resuspended in growth medium and replated at 1:2. Cells were expanded and passaged 3 times before separating GFP[+] from GFP^{−} cells by fluorescence-activated cell sorting (FACS) using a FACS Aria III flow cytometer at Purdue's Bindley Bioscience Center. GFP^{+} cells were cultured in growth medium with 4 ng/ml recombinant murine FGF-2 (PeproTech) and GFP^{−} cells were cultured in growth medium alone, both at 37°C in a humidified 5% CO_2 incubator. Sorted cells were expanded until 80–90% confluent and then passaged by dissociating cell monolayers with 1.5 mL trypsin/EDTA, centrifuged, and resuspended in growth medium and replated at 1:2. Cells were expanded and passaged a maximum of 4–5 times prior to any experiment.

Trypsinization can cause proteolytic breakdown of functional integrins on the cell membrane [49], causing a detriment to cell and ECM-derived peptide interaction. Therefore, before any cell-based experiment, cell monolayers were dissociated with 10mM EDTA in Milli-Q water with an adjusted pH of 7.4, centrifuged, and resuspended in advanced DMEM supplemented with 1% FBS, 1% L-Glutagro, and 1% Penicillin-Streptomycin. The advanced DMEM allows for a significant reduction in serum while maintaining the same growth rate/ morphology as that seen using high (10%) serum. This media was used to minimize the effect that serum proteins could have on cell adhesion to HA hydrogels and peptides.

2.5.2   Cell migration—Each cell subpopulation was seeded on the surface of 1%, 2% or 3% (w/v) HA hydrogels previously formed in a μ-slide angiogenesis slide, at a density of 5,000 cells/cm². Cells were allowed to attach and equilibrate at 37°C in a 5% CO_2 on a Leica DMI6000 fluorescent microscope equipped with a PECON BLX Black Incubator for

3 h, followed by time-lapse imaging with a frequency of 1 image per hour for 24 h, at 5×. Individual cell migration was quantified over the first 12 h using the Manual Tracking plugin in FIJI.

2.5.3. Cell proliferation—Cells were plated on 1% 2% or 3% (w/v) HA hydrogels at a density of 5,000 cells/cm^2 and cultured for 3 h at 37 °C in a humidified 5% CO_2 incubator. Half of the media of each well was then carefully pipetted out. Then, 1 mM of 5-ethynyl-2'-deoxyuridine (EdU) with 1× PBS was diluted in growth medium to a concentration of 2 μM, and added to each well (final concentration of EdU = 1 μM). Cells were cultured for 24 h and then fixed in 4% paraformaldehyde (Sigma) for 20 min, rinsed in PBS, permeabilized with 0.5% Triton X-100 (Amersham Life Science) in PBS for 10 min and then rinsed in PBS. Cells were blocked for 15 min [blocking buffer: 20% goat serum, 0.2% bovine serum albumin (Sigma) in PBS] then rinsed with PBS three times. DNA that incorporated EdU was labeled using the Alexa Fluor 555 picolyl-azide toolkit following manufacturer's instructions. Afterwards, all nuclei were stained with 1:500 DAPI (1 mM) in PBS for 10 min. The entire well was imaged with a tile scan at 5× using a Leica DMI6000 and the number of cells actively synthesizing DNA was quantified by dividing the number of nuclei with EdU incorporation by the total number of nuclei visualized with DAPI.

2.6 Gene expression analysis

Cells were seeded on the surface of 1%, 2% or 3% (w/v) HA hydrogels on a 48-well plate at a density of 5,000 cells/cm^2. RNA was isolated according to manufacturer's instructions using a Qiagen miRNA kit. Total RNA was converted to cDNA using iScript cDNA synthesis kit (Bio-Rad) using a CFX96 real-time PCR detection system (Bio-Rad). Quantitative PCR (qPCR) was performed using SsoAdvanced Universal SYBR Green Supermix (Bio-Rad) using a CFX96. Changes in relative expression for the genes of interest were calculated using GAPDH as reference gene. Primer sequences for target genes are listed in Table 2.

2.7 Statistical analysis

Results are presented as mean ± standard deviation (SD). Statistical analysis was performed using Graphpad Prism 7 (La Jolla, Ca). Two-way ANOVA and Tukey's post hoc test were used to assess the effect of peptide and %HA on storage and loss moduli, cell migration, DNA synthesis, and gene expression. One-way ANOVA and Tukey's post hoc tests were used to assess differences in pore size across the different %HA hydrogels. In general, the sample size consisted of three independent experiments with at least three technical replicates each. Statistical significance was considered at a value of α<0.05, and statistical significance is represented as follows: *p<0.05, **p<0.01, ***p<0.001.

3. Results

3.1 Characterization of peptide-functionalized hydrogels

To examine how the mechanical properties of hydrogels were influenced by HA concentration and peptide addition, gels were tested using oscillatory shear. The linear viscoelastic range of the hydrogels was determined from angular frequency sweeps (0.1–200

rad/sec). A 0.5% strain produced constant storage modulus (G') values indicating that the samples were independent of the applied angular frequency (up to 10 rad/sec). Therefore, an angular frequency of 1 rad/sec was used to determine G' by testing hydrogels with an oscillatory stress sweep ranging from 0.1 – 100 Pa. G' was compared between samples at an oscillatory stress of 10 Pa (Fig. 1). As expected, G' significantly increased as HA concentration increased from 1% to 3% ($p < 0.05$; Fig. 1A). Notably, G' was much higher than the loss modulus (G'') at all HA concentrations, demonstrating that the rheological response was dominated by the elastic behavior (Fig. 1B). To assess if peptide addition had an impact on mechanical properties, hydrogels were functionalized with up to 588 μM peptide, double the concentration used in subsequent studies. G' was not significantly affected by peptide functionalization (Fig. 1C).

To study the inner structure, the pore structure of the hydrogels was resolved by cryo-SEM. A honeycomb pore structure was revealed that significantly decreased in pore diameter as %HA increased ($p < 0.001$; Fig. 2). Functionalization with peptide did not affect pore diameter (Fig. 2B).

3.2 Peptide type and %HA have a significant effect on GFP⁺ and GFP⁻ cell proliferation

Fibrotic tissue formation is thought to be caused by excessive expansion of connective tissue cells over MPCs at the site of injury [18]. Therefore, we determined the influence of %HA and different ECM-derived peptides on proliferation by quantifying the number of cells that were actively synthesizing DNA. In order to separately analyze the effect of %HA and peptide type on the behavior of satellite and connective tissue cells, we used a mouse model in which muscle progenitors were labeled with GFP [50]. Cells were isolated from tibialis anterior muscles of Pax3-Cre/ZsGreen1 mice using collagenase and sorted using FACS to generate two different cell populations: GFP⁺ (MPCs) and GFP⁻ (connective tissue cells). Unless specified, data was normalized to the 1% HA peptide-free hydrogels.

Overall, the HA hydrogels stimulated higher DNA synthesis in GFP⁺ cells than the GFP⁻ cells (Fig. 3). The highest amount of DNA synthesized was found on cells plated on 2% HA functionalized with RGD. Variations in %HA in the peptide-free hydrogels did not have a significant impact on DNA synthesis of GFP⁻ cells (Fig. 3). However, peptide-functionalized 3% HA hydrogels induced a significant increase in DNA synthesis by GFP⁻ cells compared with the other percentages ($p < 0.05$).

Taken together, DNA synthesis by GFP⁻ cells is upregulated regardless of the peptide type used in this study, as long as higher %HA hydrogels are used. Meanwhile, DNA synthesis of GFP⁺ cells was specifically stimulated on the 2% HA hydrogel functionalized with RGD ($p < 0.05$).

3.3 Peptide type and %HA affects cell migration

In addition to proliferation, satellite cell migration to the site of injury is critical for the promotion of muscle repair. Therefore, the influence of %HA and ECM-derived peptides on the migration of FACS isolated GFP⁺ and GFP⁻ cells was determined. Overall, the total distance traveled by GFP- cells was of a similar magnitude as GFP⁺ cells (Fig. 4); however, the migratory response was less affected by %HA. The addition of RGD decreased

migration of both GFP$^+$ and GFP$^-$ cells on 2 and 3% HA compared to not only 1% HA functionalized with RGD (p < 0.001), but also all other hydrogel-peptide combinations (Fig. 4). Interestingly, the combination of %HA and IKVAV had opposite effect on the migratory response of the two cell types. While the increase in %HA accompanied with IKVAV incorporation enhanced GFP$^+$ cell migration (p < 0.001), a significant reduction in GFP$^-$ cell migration was observed (p < 0.05).

Taken together, GFP$^+$ cell migration showed more sensitivity to changes in %HA and type of peptide, whereas GFP$^-$ cell migration was mainly affected by type of peptide. The latter can be confirmed by noting no difference in GFP$^-$ cell migration on peptide-free hydrogels, while GFP$^+$ migratory response was significantly affected by %HA within each peptide group.

3.4 Hydrogel mechanical properties along with RGD and IKVAV incorporation enhanced cell spreading

Cell attachment and cell spreading correlates with increased cell viability and proliferation [51]. Therefore, promotion of cell attachment and spreading by ECM-derived peptides on GFP$^+$ and GFP$^-$ cells on the hydrogels was assessed after 24 h. Overall, GFP$^+$ and GFP$^-$ cells spread more on the HA hydrogels functionalized with RGD and IKVAV in comparison to TN-C and peptide-free hydrogels. Interestingly, cluster formation seen on the peptide-free hydrogels was diminished only on the 2% HA hydrogels for both GFP$^+$ and GFP$^-$ cells (Figs. 5, 6). As seen on the peptide-free hydrogels, differences in cell spreading and intercellular binding were seen across the different %HA hydrogels functionalized with either RGD or IKVAV. Of note, for GFP$^+$ cells, both 2% and 3% HA hydrogels enhanced cell spreading in a similar way among hydrogels with RGD or IKVAV incorporation. However, GFP$^-$ cells were more susceptible to changes in %HA. IKVAV promoted higher cell spreading on the 2% HA hydrogels while RGD incorporation enhanced cell spreading on the 3% HA hydrogels (Fig. 6).

3.5 Myod1 and Pax7 are significantly upregulated by IKVAV on the 3% HA hydrogels

In mature muscle, satellite cells reside in a quiescent form, identified by the expression of the transcription factor paired box 7 (Pax7) [52]. In response to extrinsic signals, such as changes in the myofiber ECM during muscle repair, satellite cells become activated and upregulate the expression of myogenic regulatory factors (MRFs), including myogenic factor 5 (Myf5), myogenic differentiation 1 (Myod1), and myogenin (Myog) [52]. First, satellite cells proliferate to generate a heterogeneous population of progenitors, some of which only express Pax7 and will eventually repopulate the satellite cell niche, and others that co-express Myf5 and/or Myod1. These Pax7$^+$Myf5$^+$Myod1$^+$ cells proliferate to generate a population of MPCs that will restore functionality to damaged muscle. Myf5 is correlated with satellite cell self-renewal, whereas Myod1 promotes both proliferation and commitment towards differentiation. Myod1 induces the expression of Myog, which in turn downregulates Pax7 and Myf5 and drives MPC fusion with damaged myofibers or with each other [52].

Therefore, we analyzed how expression of *Pax7* and the myogenic factors involved in satellite self-renewal (*Myf5*), cell activation (*Myod1*), and differentiation (*Myog*) were affected by %HA and type of peptide on GFP^{+} cells. Gene expression was assessed at 24 h post cell seeding. Significant differences were found only in *Myod1* and *Pax7*, where both genes were significantly upregulated on the 3% HA hydrogel peptide-free and 3% HA hydrogel functionalized with IKVAV (Fig. 7).

4. Discussion

Providing the necessary framework to sustain coordinated cell migration, viability, and proliferation is critical for promoting muscle regeneration after VML. Even though fibroblast synthesis of ECM is an important step for muscle regeneration, a regulated expansion of these cells and the enrichment of MPCs at the site of injury is needed to avoid fibrotic tissue formation [13, 24]. HA upregulation has been correlated with numerous cell responses, from promoting cell proliferation to stimulating cell motility [25, 53]. In this study, we analyzed the effect of HA-based scaffold stiffness and the influence of ECM-derived peptides from proteins upregulated during muscle injury on myogenic and connective tissue cell behavior with the purpose of providing information to better engineer a scaffold for VML repair. To assess the effect of stiffness of HA based scaffolds, the weight percent of HA in the network was varied, resulting in significant increases in the storage modulus (Fig. 1). Overall, the HA based hydrogels promoted higher proliferation of MPCs in comparison with connective tissue cells (Fig. 3), indicating HA scaffold stiffness is an important parameter to control for VML repair.

To increase cell adhesion, HA hydrogels were functionalized at the same peptide concentration with either a fibronectin, a TN-C or a laminin peptide and the influence on myogenic and connective tissue cell response was assessed. FN is one of the first ECM proteins upregulated upon muscle injury and thought to providing a support framework, enabling satellite cell proliferation at the site of injury [54]. To this end we incorporated RGD, a well-known sequence present in FN. Interestingly, RGD significantly enhanced GFP[+] cell proliferation on the 2% HA hydrogels with G' of 1.7kPa. The down regulation of DNA synthesis on the 3% HA hydrogels functionalized with RGD could be caused by the induction of satellite cell differentiation on substrates with higher stiffness, correlating with past studies showing that changes in stiffness control satellite cell fate [20, 38]. In addition, the expression of genes correlated with differentiation, *Myod1* and *Myog*, showed an overall, though not significant, increase between 2 and 3% HA (Fig. 7), which may also act to limit cell cycle reentry. With respect to GFP^{−} cells, RGD was the only peptide able to significantly stimulate DNA synthesis on the 2% HA hydrogels to similar levels as the stiffest peptide-functionalized 3% HA hydrogels. Interestingly, functionalization of the 3% HA hydrogels stimulated DNA synthesis by GFP^{−} cells regardless of the ECM-based peptide used in this study. The latter not only correlates with previous studies in which stiffer scaffolds promoted greater fibroblast proliferation [55], but also supports previous *in vivo* investigations that stiffness contributes to connective tissue cell over-proliferation at the site of injury compared to myogenic cell proliferation [56, 57].

Recruitment of MPCs over fibroblasts within the scaffold affects the number of available myogenic cells for muscle regeneration. Promoting adequate satellite cell migration at the site of injury will enable cells to successfully populate the entire defect for effective muscle regeneration [13]. Our data support previous findings that HA, TN-C and laminin enhance muscle cell migration [8, 12, 58]. The influence of HA on myoblast cell motility is thought to be mediated through the main hyaladherins CD44 and RHAMM [29]. The TN-C peptide, VFDNFVLK stimulates cell migration through the $\alpha7\beta1$ integrin [42], which is highly expressed in myogenic cells [59]. While GFP[+] cell migration on IKVAV-functionalized hydrogels increased as stiffness increased, cells on VFDNFVLK did not follow the same trend (Fig. 4A). In contrast, GFP[−] cell migration on IKVAV-functionalized gels decreased as stiffness increased, similar to what was observed by both populations of cells on RGD-functionalized HA (Fig. 4). These data indicate that the way in which cells respond to changes in stiffness is dependent on ECM composition. Generalizations about cell response to stiffness cannot be assumed and must be experimentally determined for each cell type, stiffness and ECM combination. Alternatively, cell behavior may be affected by ligand presentation. Even though the concentration of peptide is unchanged across the three different percentages, the pore size becomes smaller as %HA increases. Reduction in pore size diameter could bring peptides closer together allowing a single cell to interact with more binding sites, affecting cell-matrix interaction [60]. For this reason, varying peptide concentration will also likely affect cell behavior as a function of %HA. In this study, we chose a concentration above which cell morphology remained consistent across different %HA for a given peptide; however, additional studies should be conducted to fully understand the effect of ligand density, combined with %HA, on cell behavior in this system.

Consistent with past reports showing that the polyanionic properties of HA decreases cell adhesion [30], both cell types seeded on the peptide-free hydrogel maintained a clustered phenotype, confirming the need for peptide functionalization to enhance cell adhesion. HA and TN-C upregulation are thought to inhibit muscle differentiation [8], which could be the reason why peptide-free and TN-C-functionalized hydrogels inhibited cell spreading since cell-cell contact is necessary for cell fusion. In contrast, spreading was promoted on hydrogels functionalized with RGD or IKVAV peptides. Differences in cell spreading were observed across different %HA, highlighting the influence of the external mechanical environment on cells. Increased cell spreading and cell-cell interactions were noticeable on HA hydrogels functionalized with RGD, especially on the stiffer substrate, 3% hydrogel, for GFP^{−} cells (Fig. 7). The latter agrees with findings demonstrating that FN highly promotes connective tissue cell adhesion and spreading [61]. HA hydrogels functionalized with either RGD or IKVAV both promoted cell spreading of GFP^{+} cells (Fig. 6); however, these peptides induced a differential migratory response (Fig. 4). Cells on fibronectin have been described to form strong focal adhesions [62], which are accompanied by the formation of organized α-actinin, enabling the cell to be in a stabilized elongated conformation, thereby decreasing cell motility [63, 64]. In contrast, cells on laminin had less dense focal complexes with lower levels of vinculin and poorly organized α-actinin enabling greater cell motility [62, 63]. The latter could explain why IKVAV incorporation enhanced cell spreading while maintaining a locomotory advantage over RGD.

Quiescent satellite cells express the transcription factor Pax7, and upon injury are activated and express both Myod1 and Pax7 [65]. In our study, both genes were significantly upregulated on the peptide-free and IKVAV-functionalized 3% HA hydrogels. Myod1 upregulation has been correlated with myogenic cell proliferation and differentiation. However, as shown in our results it seems that expression of Myod1 during early stages are also correlated with increase myogenic cell migration. As for *Myf5* expression, a similar trend to *Myod1* was observed. However, for both *Myf5* and *Myod1*, 24 h might be too early to see any significant difference, especially for *Myog* since it is a myogenic factor that is typically not upregulated until later phases of satellite cell differentiation[52].

While proliferation was not substantially enhanced by the addition of different peptides, growth factors present at the site of injury could help mediate proliferation. Since satellite cell proliferation is highly stimulated by growth factors that are upregulated at the site of injury, including hepatocyte growth factor and insulin-like growth factor [66, 67]. Therefore, we expect that upon implantation, the *in vivo* response to hydrogels could stimulate proliferation to enhance the efficacy of the gels. Moreover, cell proliferation is enhanced at higher cell densities [68, 69], meaning that as satellite cell number increases due to migration, the proliferative response would likely increase as well. If the latter holds true, then differentiation and myotube formation would inherently follow [70].

To assess how stiffness and peptide functionalization differentially affected MPCs and surrounding connective tissue cells, a mouse model in which MPCs were GFP[+] was used. Studies from our lab and others previously demonstrated that GFP^{+} cells in the developing forelimb are predominantly (>90%) myoblasts, whereas the surrounding connective tissue cells express Tcf4, a marker for a subpopulation of fibroblasts [18, 29, 71]; however, the precise identity of both GFP[+] and GFP[−] cell populations remains unclear. The GFP^{−} cells are likely a heterogeneous population of cells, including fibroblasts, fibro-adipogenic precursors, and immune and endothelial cells [72], all of which are thought to contribute to muscle repair. By using FACS to enrich for these different populations [72], future studies will be able to identify how stiffness and peptide preferentially affect the gene expression and behavior of the various cells resident in skeletal muscle. Furthermore, since these non-myogenic cells are known to influence muscle differentiation [18, 73], future experiments combining different ratios of GFP[+]:GFP^{−} cells will provide insight into the mechanisms behind biomechanical regulation of muscle regeneration.

Hydrogels, such as those described in this study as well as others, show promise for treating VML. While previous studies utilized decellularized ECM from adult muscle or other tissues [24, 74], these grafts were minimally incorporated into the host and did not significantly restore functionality [75]. This is likely due to the lack of incorporation of cues present during muscle formation into these scaffolds, such as the extensive ECM remodeling that occurs during muscle development, regeneration and repair [7, 8, 29, 38]. Hydrogels made from naturally derived ECM such as alginate, chitosan and agarose have been shown to promote proliferation of encapsulated MPCs both *in vitro* and *in vivo* [24]. A benefit of these engineered hydrogels is that the mechanical properties and pore size can be tuned while the bioactivity can be customized to promote the desired behavior. For example, PEG-fibrinogen gels containing myogenic progenitors, were polymerized in situ using UV light

and formed muscle tissue that was innervated and vascularized [24]. However, even with these hydrogels, the treatments for VML are still far from restoring a human-sized injury, since therapies have failed to promote myogenic migration into the scaffolds. By identifying how different aspects of the biomechanical environment regulate cellular behaviors, we will be able to design scaffolds that better promote the complete restoration of damaged muscle.

5. Conclusions

With the overall goal of engineering a scaffold that could facilitate the migration of endogenous MPCs into and within the scaffolds to help enhance body's regenerative response for the treatment of VML, our results showed promise for the use of the 3% HA hydrogel functionalized with the laminin peptide, IKVAV. Attributions include the promotion of GFP$^+$ cell attachment and spreading, promotion of migration over GFP$^-$ cells, enhancement of proliferation and the upregulation of transcription factors associated with MPCs, *Myod1* and *Pax7*, for muscle repair.

Acknowledgements

Abbreviations:

cryo-SEM	cryo-scanning electron microscopy
ECM	extracellular matrix
FACS	fluorescence-activated cell sorting
FN	fibronectin
GFP	green fluorescent protein
HA	hyaluronic acid
PEGDA	poly(ethylene glycol diacrylate)
TN-C	tenascin-C
VML	volumetric muscle loss

References

[1]. Sanes JR, The basement membrane/basal lamina of skeletal muscle, J Biol Chem 278(15) (2003) 12601–4. [PubMed: 12556454]

[2]. Kjaer M, Role of extracellular matrix in adaptation of tendon and skeletal muscle to mechanical loading, Physiol Rev 84(2) (2004) 649–98. [PubMed: 15044685]

[3]. Grounds MD, Complexity of extracellular matrix and skeletal muscle regeneration, in: Schiaffino S, Partridge T (Eds.), Skeletal Muscle Repair and Regeneration, Springer, Netherlands, 2008, pp. 269–301.

[4]. Okita M, Yoshimura T, Nakano J, Motomura M, Eguchi K, Effects of reduced joint mobility on sarcomere length, collagen fibril arrangement in the endomysium, and hyaluronan in rat soleus muscle, J Muscle Res Cell Motil 25(2) (2004) 159–66. [PubMed: 15360131]

[5]. Rayagiri SS, Ranaldi D, Raven A, Mohamad Azhar IF, Lefebvre O, Zammit PS, Borycki AG, Basal lamina remodeling at the skeletal muscle stem cell niche mediates stem cell self-renewal, Nat Comm 9(1075) (2018).

[6]. Vracko R, Basal lamina scaffold-anatomy and significance for maintenance of orderly tissue structure, Am J Pathol 77(2) (1974) 314–46. [PubMed: 4614671]

[7]. Calve S, Isaac J, Gumucio JP, Mendias CL, Hyaluronic acid, HAS1, and HAS2 are significantly upregulated during muscle hypertrophy, Am J Physiol – Cell 303(5) (2012) C577–88.

[8]. Calve S, Odelberg SJ, Simon HG, A transitional extracellular matrix instructs cell behavior during muscle regeneration, Dev Biol 344(1) (2010) 259–71. [PubMed: 20478295]

[9]. Elson HF, Ingwall JS, The cell substratum modulates skeletal muscle differentiation, J Supramol Struct 14(3) (1980) 313–28. [PubMed: 7218800]

[10]. Kujawa MJ, Tepperman K, Culturing chick muscle cells on glycosaminoglycan substrates: attachment and differentiation, Dev Biol 99(2) (1983) 277–86. [PubMed: 6413281]

[11]. Jarvinen TA, Kannus P, Jarvinen TL, Jozsa L, Kalimo H, Jarvinen M, Tenascin-C in the pathobiology and healing process of musculoskeletal tissue injury, Scand J Med Sci Sports 10(6) (2000) 376–82. [PubMed: 11085568]

[12]. Mackey AL, Brandstetter S, Schjerling P, Bojsen-Moller J, Qvortrup K, Pedersen MM, Doessing S, Kjaer M, Magnusson SP, Langberg H, Sequenced response of extracellular matrix deadhesion and fibrotic regulators after muscle damage is involved in protection against future injury in human skeletal muscle, FASEB J 25(6) (2011) 1943–59. [PubMed: 21368102]

[13]. Goetsch K, Myburgh K, Niesler CU, In vitro myoblast motility models: investigating migration dynamics for the study of skeletal muscle repair, J. Muscle Res Cell Motil 2013, pp. 333–347. [PubMed: 24150600]

[14]. Patton BL, Miner JH, Chiu AY, Sanes JR, Distribution and function of laminins in the neuromuscular system of developing, adult, and mutant mice, J Cell Biol 139(6) (1997) 1507–21. [PubMed: 9396756]

[15]. Tedesco FS, Dellavalle A, Diaz-Manera J, Messina G, Cossu G, Repairing skeletal muscle: regenerative potential of skeletal muscle stem cells, J Clin Invest 120(1) (2010) 11–9. [PubMed: 20051632]

[16]. Bigard A-X, Fink E, Skeletal Muscle Regeneration After Injury: Cellular and Molecular Events, In: Rehabilitation of Sports Injuries: Scientific Basis, Ed: Frontera WR (2008) 28–55.

[17]. Grogan BF, Hsu JR, Skeletal Trauma Research C, Volumetric muscle loss, J Am Acad Orthop Surg 19 Suppl 1 (2011) S35–7. [PubMed: 21304045]

[18]. Murphy MM, Lawson JA, Mathew SJ, Hutcheson DA, Kardon G, Satellite cells, connective tissue fibroblasts and their interactions are crucial for muscle regeneration, Development 138(17) (2011) 3625. [PubMed: 21828091]

[19]. Branton MH, Kopp JB, TGF-beta and fibrosis, Microbes Infect 1(15) (1999) 1349–65. [PubMed: 10611762]

[20]. Serrano AL, Mann CJ, Vidal B, Ardite E, Perdiguero E, Munoz-Canoves P, Cellular and molecular mechanisms regulating fibrosis in skeletal muscle repair and disease, Curr Top Dev Biol 96 (2011) 167–201. [PubMed: 21621071]

[21]. Corona BT, Rivera JC, Owens JG, Wenke JC, Rathbone CR, Volumetric muscle loss leads to permanent disability following extremity trauma, J Rehabil Res Dev 52(7) (2015) 785–92. [PubMed: 26745661]

[22]. VanDusen KW, Syverud BC, Williams ML, Lee JD, Larkin LM, Engineered skeletal muscle units for repair of volumetric muscle loss in the tibialis anterior muscle of a rat, Tissue Eng Pt A 20(21–22) (2014) 2920–30.

[23]. Hodgetts SI, Beilharz MW, Scalzo AA, Grounds MD, Why do cultured transplanted myoblasts die in vivo? DNA quantification shows enhanced survival of donor male myoblasts in host mice depleted of CD4+ and CD8+ cells or Nk1.1+ cells, Cell Transplant 9(4) (2000) 489–502. [PubMed: 11038066]

[24]. Fuoco C, Petrilli LL, Cannata S, Gargioli C, Matrix scaffolding for stem cell guidance toward skeletal muscle tissue engineering, J Orthop Surg Res 11(1) (2016) 86. [PubMed: 27460672]

[25]. Collins MN, Birkinshaw C, Hyaluronic acid based scaffolds for tissue engineering--a review, Carbohyd Polym 92(2) (2013) 1262–79.

[26]. Shu XZ, Liu Y, Luo Y, Roberts MC, Prestwich GD, Disulfide cross-linked hyaluronan hydrogels, Biomacromolecules 3(6) (2002) 1304–11. [PubMed: 12425669]

[27]. Zheng Shu X, Liu Y, Palumbo FS, Luo Y, Prestwich GD, In situ crosslinkable hyaluronan hydrogels for tissue engineering, Biomaterials 25(7–8) (2004) 1339–48. [PubMed: 14643608]

[28]. Zhu J, Bioactive modification of poly(ethylene glycol) hydrogels for tissue engineering, Biomaterials 31(17) (2010) 4639–56. [PubMed: 20303169]

[29]. Leng Y, Abdullah A, Wendt MK, Calve S, Hyaluronic acid, CD44 and RHAMM regulate myoblast behavior during embryogenesis, Matrix Biol (2018) DOI: 10.1016/j.matbio.2018.08.008.

[30]. Shu XZ, Ghosh K, Liu Y, Palumbo FS, Luo Y, Clark RA, Prestwich GD, Attachment and spreading of fibroblasts on an RGD peptide-modified injectable hyaluronan hydrogel, J Biomed Mater Res A 68(2) (2004) 365–75. [PubMed: 14704979]

[31]. Hersel U, Dahmen C, Kessler H, RGD modified polymers: biomaterials for stimulated cell adhesion and beyond, Biomaterials 24(24) (2003) 4385–415. [PubMed: 12922151]

[32]. Rossi CA, Flaibani M, Blaauw B, Pozzobon M, Figallo E, Reggiani C, Vitiello L, Elvassore N, De Coppi P, In vivo tissue engineering of functional skeletal muscle by freshly isolated satellite cells embedded in a photopolymerizable hydrogel, FASEB J 25(7) (2011) 2296–304. [PubMed: 21450908]

[33]. Desiderio V, De Francesco F, Schiraldi C, De Rosa A, La Gatta A, Paino F, d'Aquino R, Ferraro GA, Tirino V, Papaccio G, Human Ng2+ adipose stem cells loaded in vivo on a new crosslinked hyaluronic acid-Lys scaffold fabricate a skeletal muscle tissue, J Cell Physiol 228(8) (2013) 1762–73. [PubMed: 23359523]

[34]. Wang W, Fan M, Zhang L, Liu SH, Sun L, Wang CY, Compatibility of hyaluronic acid hydrogel and skeletal muscle myoblasts, Biomed Mater 4(2) (2009) 025011. [PubMed: 19258701]

[35]. Flaibani M, Elvassore N, Gas anti-solvent precipitation assisted salt leaching for generation of micro- and nano-porous wall in bio-polymeric 3D scaffolds, Mater Sci Eng C Mater Biol Appl 32(6) (2012) 1632–9. [PubMed: 24364970]

[36]. Bencherif SA, Srinivasan A, Horkay F, Hollinger JO, Matyjaszewski K, Washburn NR, Influence of the degree of methacrylation on hyaluronic acid hydrogels properties, Biomaterials 29(12) (2008) 1739–49. [PubMed: 18234331]

[37]. Poveda-Reyes S, Moulisova V, Sanmartin-Masia E, Quintanilla-Sierra L, Salmeron-Sanchez M, Ferrer GG, Gelatin-hyaluronic acid hydrogels with tuned stiffness to counterbalance cellular forces and promote cell differentiation, Macromol Biosci 16(9) (2016) 1311–24. [PubMed: 27213762]

[38]. Calve S, Simon HG, Biochemical and mechanical environment cooperatively regulate skeletal muscle regeneration, FASEB J 26(6) (2012) 2538–45. [PubMed: 22415307]

[39]. Gilbert PM, Havenstrite KL, Magnusson KE, Sacco A, Leonardi NA, Kraft P, Nguyen NK, Thrun S, Lutolf MP, Blau HM, Substrate elasticity regulates skeletal muscle stem cell self-renewal in culture, Science 329(5995) (2010) 1078–81. [PubMed: 20647425]

[40]. Sazonova OV, Isenberg BC, Herrmann J, Lee KL, Purwada A, Valentine AD, Buczek-Thomas JA, Wong JY, Nugent MA, Extracellular matrix presentation modulates vascular smooth muscle cell mechanotransduction, Matrix Biol 41 (2015) 36–43. [PubMed: 25448408]

[41]. Ruoslahti E, RGD and other recognition sequences for integrins, Annu Rev Cell Dev Biol 12 (1996) 697–715. [PubMed: 8970741]

[42]. Mercado ML, Nur-e-Kamal A, Liu HY, Gross SR, Movahed R, Meiners S, Neurite outgrowth by the alternatively spliced region of human tenascin-C is mediated by neuronal alpha7beta1 integrin, J Neurosci 24(1) (2004) 238–47. [PubMed: 14715956]

[43]. Tashiro K, Sephel GC, Weeks B, Sasaki M, Martin GR, Kleinman HK, Yamada Y, A synthetic peptide containing the IKVAV sequence from the A chain of laminin mediates cell attachment, migration, and neurite outgrowth, J Biol Chem 264(27) (1989) 16174–82. [PubMed: 2777785]

[44]. Eng D, Caplan M, Preul M, Panitch A, Hyaluronan scaffolds: a balance between backbone functionalization and bioactivity, Acta Biomater 6(7) (2010) 2407–14. [PubMed: 20051273]

[45]. Butterworth PH, Baum H, Porter JW, A modification of the Ellman procedure for the estimation of protein sulfhydryl groups, Arch Biochem Biophys 118(3) (1967) 716–23. [PubMed: 6069104]

[46]. Ellman GL, A colorimetric method for determining low concentrations of mercaptans, Arch Biochem Biophys 74(2) (1958) 443–50. [PubMed: 13534673]

[47]. Engleka KA, Gitler AD, Zhang M, Zhou DD, High FA, Epstein JA, Insertion of Cre into the Pax3 locus creates a new allele of Splotch and identifies unexpected Pax3 derivatives, Dev Biol 280(2) (2005) 396–406. [PubMed: 15882581]

[48]. Madisen L, Zwingman TA, Sunkin SM, Oh SW, Zariwala HA, Gu H, Ng LL, Palmiter RD, Hawrylycz MJ, Jones AR, Lein ES, Zeng H, A robust and high-throughput Cre reporting and characterization system for the whole mouse brain, Nat Neurosci 13(1) (2010) 133–40. [PubMed: 20023653]

[49]. Huang HL, Hsing HW, Lai TC, Chen YW, Lee TR, Chan HT, Lyu PC, Wu CL, Lu YC, Lin ST, Lin CW, Lai CH, Chang HT, Chou HC, Chan HL, Trypsin-induced proteome alteration during cell subculture in mammalian cells, J Biomed Sci 17(1) (2010) 36. [PubMed: 20459778]

[50]. Mayeuf-Louchart A, Lagha M, Danckaert A, Rocancourt D, Relaix F, Vincent SD, Buckingham M, Notch regulation of myogenic versus endothelial fates of cells that migrate from the somite to the limb, Proc Natl Acad Sci U S A 111(24) (2014) 8844–9. [PubMed: 24927569]

[51]. Hynes RO, Cell adhesion: old and new questions, Trends Cell Biol 9(12) (1999) M33–7. [PubMed: 10611678]

[52]. Hernandez-Hernandez JM, Garcia-Gonzalez EG, Brun CE, Rudnicki MA, The myogenic regulatory factors, determinants of muscle development, cell identity and regeneration, Semin Cell Dev Biol 72 (2017) 10–18. [PubMed: 29127045]

[53]. Misra S, Hascall VC, Markwald RR, Ghatak S, Interactions between hyaluronan and its receptors (CD44, RHAMM) regulate the activities of inflammation and cancer, Front Immunol 6(MAY) (2015) 201. [PubMed: 25999946]

[54]. Bentzinger CF, Wang YX, von Maltzahn J, Soleimani VD, Yin H, Rudnicki MA, Fibronectin regulates Wnt7a signaling and satellite cell expansion, Cell Stem Cell 12(1) (2013) 75–87. [PubMed: 23290138]

[55]. Hadjipanayi E, Mudera V, Brown RA, Close dependence of fibroblast proliferation on collagen scaffold matrix stiffness, J Tissue Eng Regen Med 3(2) (2009) 77–84. [PubMed: 19051218]

[56]. Lieber RL, Ward SR, Cellular mechanisms of tissue fibrosis. 4. Structural and functional consequences of skeletal muscle fibrosis, Am J Physiol-Cell Ph 305(3) (2013) C241–52.

[57]. Mackey AL, Magnan M, Chazaud B, Kjaer M, Human skeletal muscle fibroblasts stimulate in vitro myogenesis and in vivo muscle regeneration, J Physiol 595(15) (2017) 5115–5127. [PubMed: 28369879]

[58]. Murphy-Ullrich JE, The de-adhesive activity of matricellular proteins: is intermediate cell adhesion an adaptive state?, J Clin Invest 107(7) (2001) 785–90. [PubMed: 11285293]

[59]. Boppart MD, Burkin DJ, Kaufman SJ, Alpha7beta1-integrin regulates mechanotransduction and prevents skeletal muscle injury, Am J Physiol-Cell Ph 290(6) (2006) C1660–5.

[60]. Trappmann B, Gautrot JE, Connelly JT, Strange DG, Li Y, Oyen ML, Cohen Stuart MA, Boehm H, Li B, Vogel V, Spatz JP, Watt FM, Huck WT, Extracellular-matrix tethering regulates stem-cell fate, Nat Mater 11(7) (2012) 642–9. [PubMed: 22635042]

[61]. Terranova VP, Aumailley M, Sultan LH, Martin GR, Kleinman HK, Regulation of cell attachment and cell number by fibronectin and laminin, J Cell Physiol 127(3) (1986) 473–9. [PubMed: 3711151]

[62]. Goodman SL, Risse G, von der Mark K, The E8 subfragment of laminin promotes locomotion of myoblasts over extracellular matrix, J Cell Biol 109(2) (1989) 799–809. [PubMed: 2503526]

[63]. Parsons JT, Horwitz AR, Schwartz MA, Cell adhesion: integrating cytoskeletal dynamics and cellular tension, Nat Rev Mol Cell Biol 11(9) (2010) 633–43. [PubMed: 20729930]

[64]. Rodriguez Fernandez JL, Geiger B, Salomon D, Ben-Ze'ev A, Overexpression of vinculin suppresses cell motility in BALB/c 3T3 cells, Cell Motil Cytoskeleton 22(2) (1992) 127–34. [PubMed: 1633623]

[65]. Oustanina S, Hause G, Braun T, Pax7 directs postnatal renewal and propagation of myogenic satellite cells but not their specification, EMBO J 23(16) (2004) 3430–9. [PubMed: 15282552]

[66]. Sheehan SM, Tatsumi R, Temm-Grove CJ, Allen RE, HGF is an autocrine growth factor for skeletal muscle satellite cells in vitro, Muscle & Nerve 23(2) (2000) 239–245. [PubMed: 10639617]

[67]. Machida S, Booth FW, Insulin-like growth factor 1 and muscle growth: implication for satellite cell proliferation, Proc Nutr Soc 63(2) (2004) 337–40. [PubMed: 15294052]

[68]. Tanaka K, Sato K, Yoshida T, Fukuda T, Hanamura K, Kojima N, Shirao T, Yanagawa T, Watanabe H, Evidence for cell density affecting C2C12 myogenesis: possible regulation of myogenesis by cell-cell communication, Muscle Nerve 44(6) (2011) 968–77. [PubMed: 22102468]

[69]. Krauss RS, Cole F, Gaio U, Takaesu G, Zhang W, Kang JS, Close encounters: regulation of vertebrate skeletal myogenesis by cell-cell contact, J Cell Sci 118(Pt 11) (2005) 2355–62. [PubMed: 15923648]

[70]. Cheng CS, Ran L, Bursac N, Kraus WE, Truskey GA, Cell Density and Joint microRNA-133a and microRNA-696 Inhibition Enhance Differentiation and Contractile Function of Engineered Human Skeletal Muscle Tissues, Tissue Eng Pt A 22(7–8) (2016) 573–83.

[71]. Hutcheson DA, Zhao J, Merrell A, Haldar M, Kardon G, Embryonic and fetal limb myogenic cells are derived from developmentally distinct progenitors and have different requirements for beta-catenin, Genes Dev 23(8) (2009) 997–1013. [PubMed: 19346403]

[72]. Latroche C, Weiss-Gayet M, Gitiaux C, Chazaud B, Cell sorting of various cell types from mouse and human skeletal muscle, Methods 134–135 (2018) 50–55.

[73]. Joe AW, Yi L, Natarajan A, Le Grand F, So L, Wang J, Rudnicki MA, Rossi FM, Muscle injury activates resident fibro/adipogenic progenitors that facilitate myogenesis, Nat Cell Biol 12(2) (2010) 153–63. [PubMed: 20081841]

[74]. Badylak SF, Dziki JL, Sicari BM, Ambrosio F, Boninger ML, Mechanisms by which acellular biologic scaffolds promote functional skeletal muscle restoration, Biomaterials 103 (2016) 128–136. [PubMed: 27376561]

[75]. Corona BT, Greising SM, Challenges to acellular biological scaffold mediated skeletal muscle tissue regeneration, Biomaterials 104 (2016) 238–46. [PubMed: 27472161]

Author Manuscript

Author Manuscript

Author Manuscript

Author Manuscript

Statement of Significance

The goal of this study was to identify hyaluronic acid (HA) hydrogels with peptide and stiffness combinations that will direct muscle-derived cells towards regenerating phenotypes. While the interaction of skeletal muscle with RGD-functionalized HA hydrogels has been investigated, none of the other peptides described in this study had been used in the context of HA-based scaffolds and skeletal muscle-derived cells. Notably, the response of cells to variations in mechanics was dependent on ECM coating and lineage. *The 3% HA functionalized with the laminin peptide, IKVAV, showed the most promise for future in vivo studies, as these hydrogels best promoted myoblast cell proliferation, attachment and spreading, enhanced migration over connective tissue cells and upregulated transcription factors associated with activated satellite cells.*
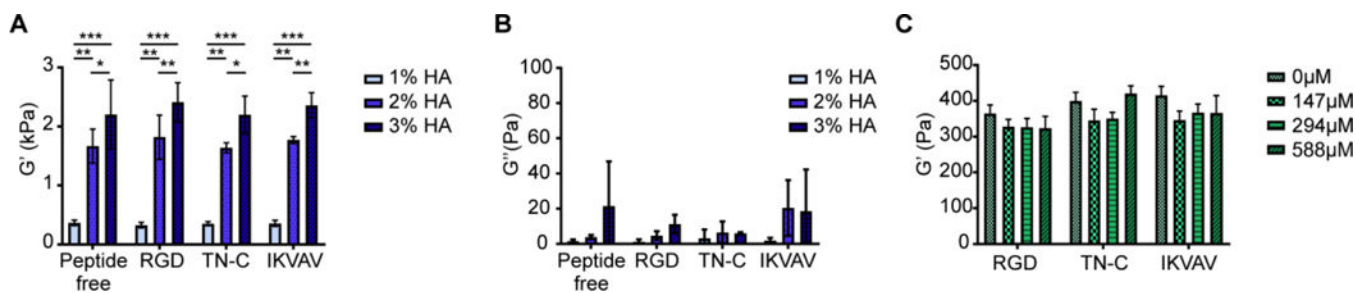
Fig. 1.
Storage modulus of HA hydrogels is not affected by peptide functionalization. (A) G'
significantly increased as HA concentration increased from 1 – 3 % (w/v). Oscillatory shear
stress was performed at 1 rad/sec and G' determined at an oscillatory shear stress of 10 Pa.
Two-way ANOVA indicated that %HA significantly affected G' ($p < 0.05$), whereas
functionalization with 294 μM peptide did not. Tukey's post-hoc test revealed significant
differences between G' of different gel percentages (*$p < 0.05$, **$p < 0.01$, ***$p < 0.001$).
(B) Loss modulus, G", was significantly lower than G' indicating that hydrogel mechanics is
dominated by the elastic behavior. Two-way ANOVA indicated significant difference
between G' and G" ($p < 0.0001$). Tukey's post-hoc test revealed significant differences
between G' and G" of the same %HA hydrogel (***$p < 0.0001$). (C) Functionalization of
1% HA with 0 – 588 μM peptide did not significantly affect G'. Error bars = SD, n = 4 for
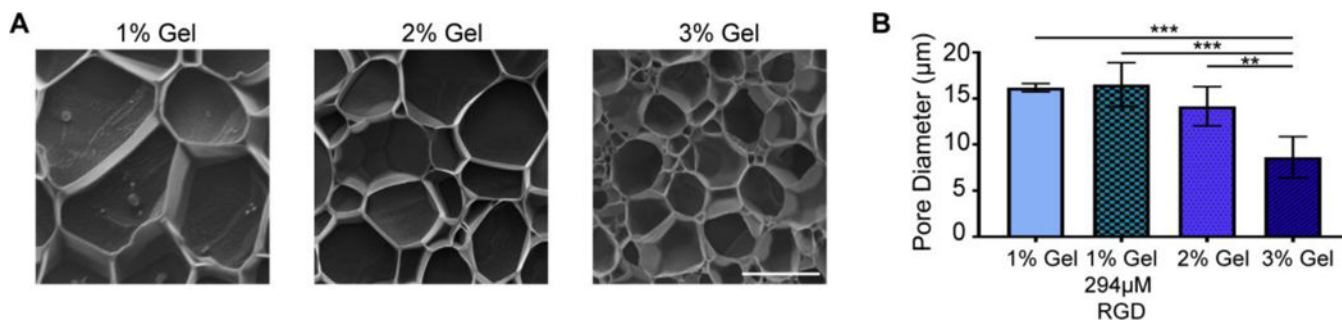each treatment.

Fig. 2.
Pore diameter of hydrogels decreases as HA percentage increases. (A) Representative cryo-SEM images for 1 – 3% HA hydrogels. Bar = 10 μm (B) One-way ANOVA indicated that pore diameter was significantly affected by HA% ($p < 0.001$). Tukey's post-hoc test revealed a significant decrease in pore diameter in the 3% HA hydrogel compared to the other hydrogels. (**$p < 0.01$, ***$p < 0.001$). HA functionalized with 294 μM RGD was also tested, indicating that functionalization did not significantly affect pore diameter. Error bars = SD, n=4 for each treatment.
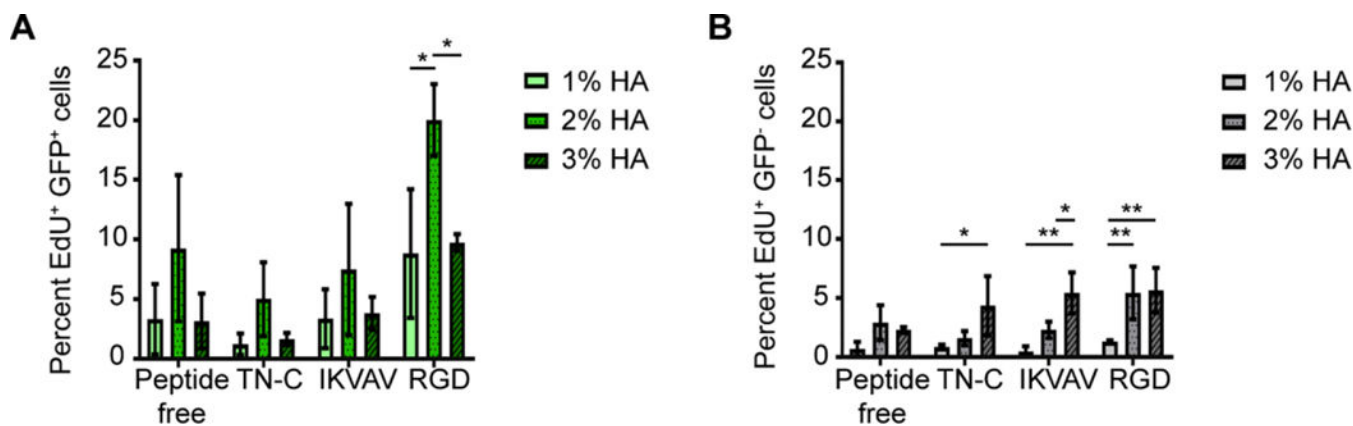
Fig. 3.
DNA synthesis by GFP$^+$ and GFP$^-$ cells is influenced by %HA and type of peptide. Overall DNA synthesis by GFP$^+$ cells was greater than that by the GFP$^-$ cells. (A) GFP$^+$ cells showed the highest DNA synthesis on the 2% HA hydrogels functionalized with RGD. Two-way ANOVA revealed significance for peptide ($p < 0.05$) and gel percentage ($p < 0.0001$). (B) Two-way ANOVA revealed significance for peptide ($p < 0.05$) and gel percentage ($p < 0.0001$) on EdU incorporation by GFP$^-$ cells. Tukey's post hoc test showed a significant increase in DNA synthesis on the 3% peptide-functionalized hydrogels compared with 1% HA. Cells were cultured *in vitro* for 24 h and the percentage of cells that synthesized new DNA was determined by labeling for EdU incorporation (*$p < 0.05$; **$p < 0.005$). Error bars = SD; n   360 cells per hydrogel combination. Three independent experiments were averaged with n   3 technical replicates per experiment.
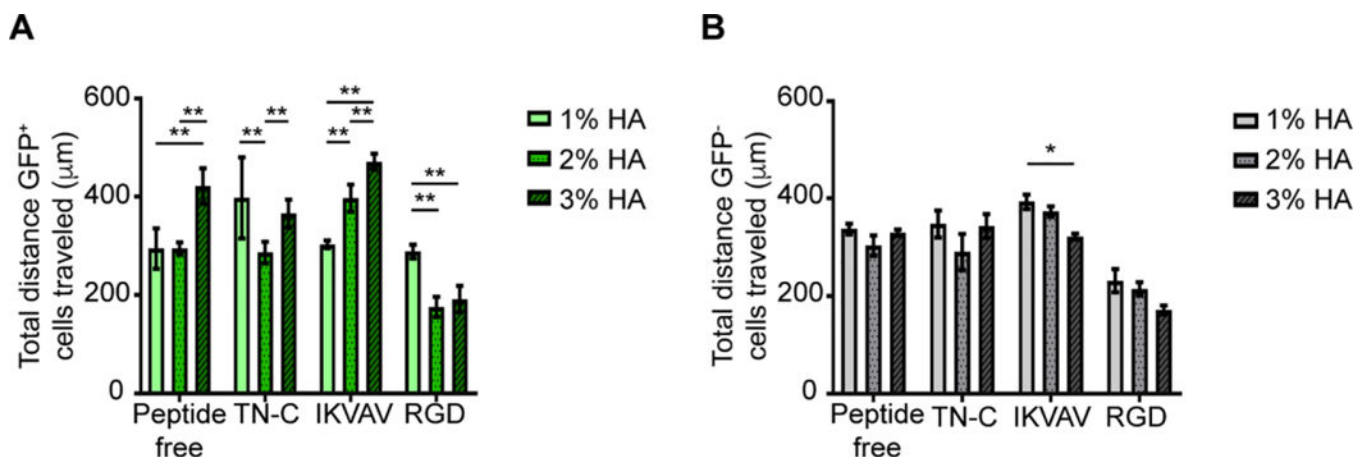
Fig. 4.
Migratory response of GFP+ and GFP− cells is influenced by %HA and type of peptide. There was an overall decrease in GFP+ and GFP− cell migration on RGD-functionalized hydrogels. While TN-C-functionalized hydrogels had a similar effect on both GFP+ and GFP− cells, IKVAV-functionalized hydrogels had an opposite effect on the migratory response of the two cell types. A) The migratory response of GFP+ cells was significantly affected by %HA within each peptide group. Two-way ANOVA showed significance for peptide/%HA interaction ($p < 0.0001$), peptide ($p < 0.0001$), and %HA ($p < 0.0001$). Tukey's post hoc test revealed the effect of %HA on the different peptide groups (*$p < 0.05$, **$p < 0.01$, ***$p < 0.001$). B) The migratory response of GFP− cells was less affected by %HA and peptide type. Two-way ANOVA showed significance for %HA ($p < 0.05$) and type of peptide ($p < 0.0001$). Tukey's post hoc test revealed difference in cell migration by IKVAV-functionalized hydrogels between 1% and 3% HA (*$p < 0.05$). GFP+ and GFP− cells were imaged and tracked every hour for 12 h. Error bars = SD; n   100 cells per %HA-peptide combination. Three independent experiments were averaged with n   3 technical replicates per experiment.
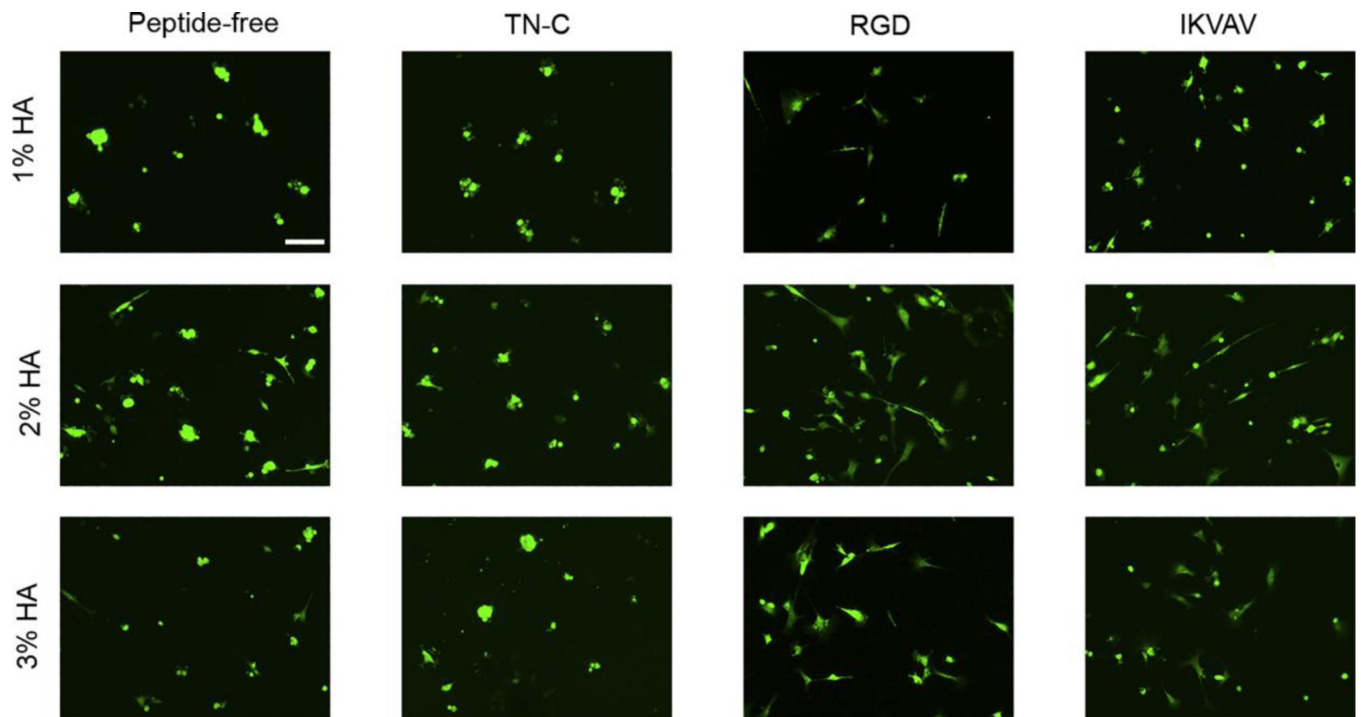
Fig. 5.

Incorporation of ECM-derived peptides and hydrogel stiffness impacts the attachment and spreading of GFP+ cells. RGD and IKVAV-functionalized hydrogels enhanced cell spreading in comparison to the cell clustering effect observed on peptide free and TN-C-functionalized hydrogels. Bar = 100 μm, 5×.
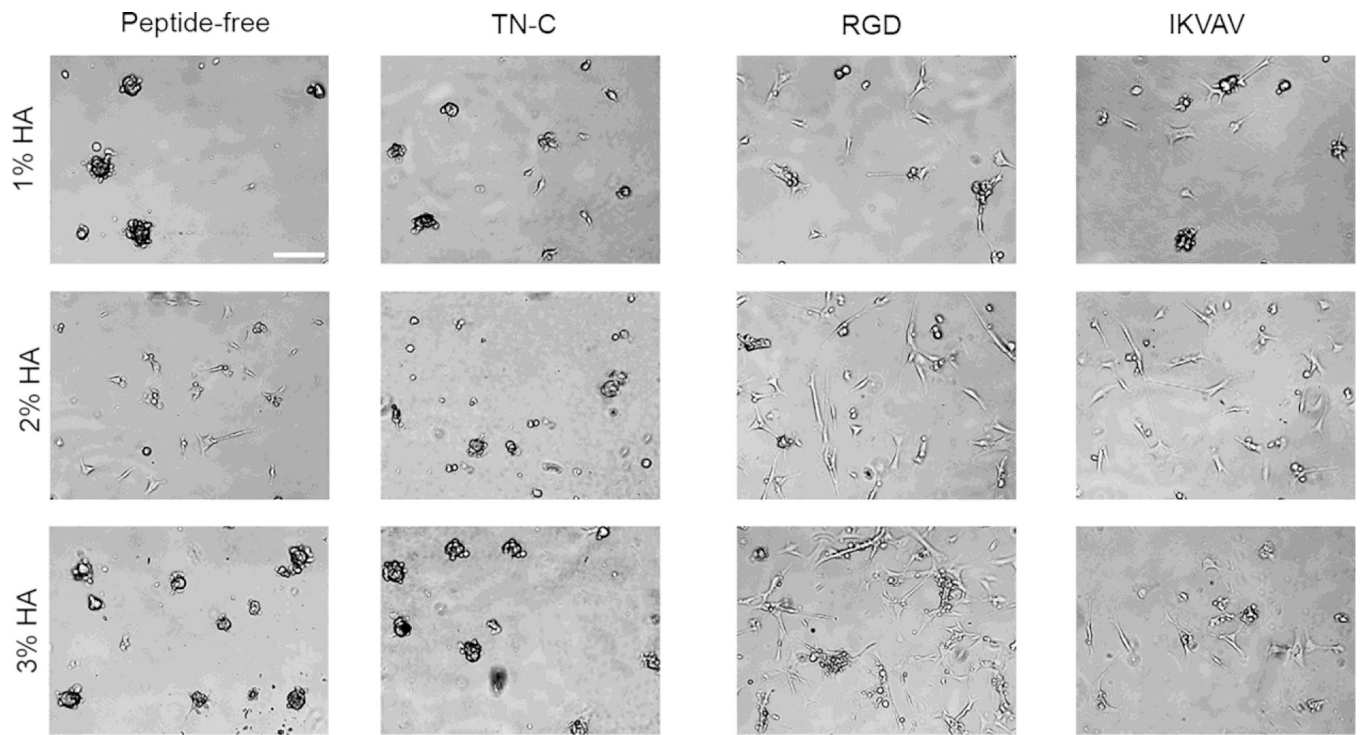
Fig. 6.
Incorporation of ECM-derived peptides and hydrogel stiffness impacts the attachment and spreading of GFP⁻ cells. Similar to GFP⁺ cells, RGD and IKVAV-functionalized hydrogels promoted higher cell attachment and cell spreading. Cell spreading was enhanced on RGD-functionalized hydrogels as gel percentage increased. In comparison, peptide-free and IKVAV-functionalized hydrogels promoted higher cell spreading on the 2% HA hydrogel. Bar = 100 μm, 5×.
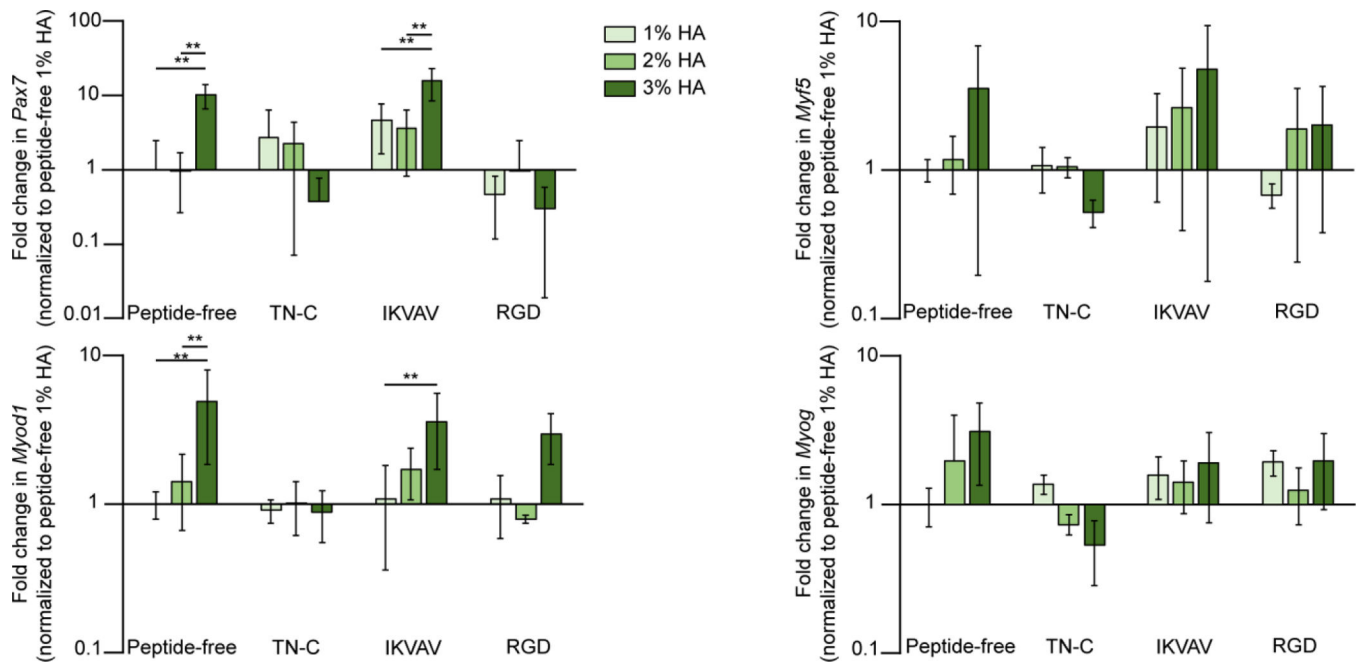
Fig. 7.
Myod1 and *Pax7* were highly upregulated on peptide-free and IKVAV functionalized 3% HA hydrogels. *Myod1* Two-way ANOVA showed significance for %HA (p < 0.01). Pax7 Two-way ANOVA showed significance for %HA (p < 0.01) and type of peptide (p < 0.01). Tukey's post hoc test revealed the effect of %HA on the peptide-free and IKVAV functionalized hydrogels for *Myod1* and *Pax7* (*p < 0.05; **p < 0.005). Error bars = SD; three independent experiments were averaged with n ≥ 3 technical replicates per experiment.

Table 1.

ECM-derived peptides used in the study

	Peptide sequence	Reference
Fibronectin	Cys-Gly-Arg-Gly-Asp-Ser (CGRGDS)	[41]
Tenascin-C	Val-Phe-Asp-Asn-Phe-Val-Leu-Lys-Gly-Ser-Cys (VFDNFVLKGSC)	[42]
Laminin	Cys-Ser-Gly-Ile-Lys-Val-Ala-Val (CSGIKVAV)	[43]

Table 2.

Primer sequences for qPCR analysis.

Gene	Forward Primer 5′–3′	Reverse Primer 5′–3′	size, bp	Ref Seq
Pax7	GAATCAGAACCCGACCTCCC	CGCCGGTTACTGAACCAGA	191	NM_011039.2
Myod1	GAACCCAACCTGAACGTCTG	GTGTGGCCGCCATTCTTTATC	91	NM_010783.3
Myog	GCAGGCTCAAGAAAGTGAATGA	TAGGCGCTCAATGTACTGGAT	122	NM_001164048.1
Myf5	AAGGCTCCTGTATCCCCTCAC	TGACCTTCTTCAGGCGTCTAC	249	NM_008656.5
Gapdh	TGGAAAGCTGTGGCGTGAT	TGCTTCACCACCTTCTTGAT	216	NM_008084.2